Contrib Mineral Petrol (1997) 126: 224 – 236

Richard A. Yund

Rates of grain boundary diffusion through enstatite and forsterite reaction rims

Received: 1 July 1995 / Accepted: 1 August 1996

Abstract The growth rates of enstatite rims produced by reaction of Fo_{92} and SiO_2 were determined at 250–1500 MPa and 900–1100°C for a wide range of water contents. Growth rates were also determined for forsterite rims between MgO and $Mg_2Si_2O_6$ and between MgO and SiO_2. Rim growth rates are parabolic indicating diffusion-controlled growth of the polycrystalline rims which are composed of ~ 2 μm diameter grains. Rim growth rates were used to calculate the product of the grain boundary diffusion coefficient (D'_A) times the effective grain boundary thickness (δ) assuming in turn that MgO, SiO_2, and Mg_2Si_{-1} are the diffusing components (coupled diffusion of a cation and oxygen or interdiffusion of Mg and Si). The values for $D'_{MgO}\delta$, $D'_{SiO_2}\delta$, and $D'_{Mg_2Si-1}\delta$ for enstatite at 1000°C and 700 MPa confining pressure with about 0.1 wt % water are about five times larger than the corresponding $D'_A\delta$ values for samples initially vacuum dried at 250°C. Most of the increase in $D'_A\delta$ occurs with the first 0.1 wt % water. The activation energy for diffusion through the enstatite rims (1100–950°C) is 162 ± 30 kJ/mole. The diffusion rate through enstatite rims is essentially unchanged for confining pressures from 210–1400 MPa, but the nucleation rate is greatly reduced at low confining pressure (for ≤ 1.0 wt % water present) and limits the conditions at which rim growth can be measured. The corresponding values for $D'_A\delta$ through forsterite rims are essentially identical for the two forsterite-producing reactions when 0.1 wt % water is added and similar to the $D'_A\delta$ values for enstatite at the same conditions. The $D'_A\delta$ values for forsterite are ~ 28 times larger for samples starting with 0.1 wt % water compared to samples that were first vacuum dried. Thus water enhances these grain boundary diffusion rates by a factor of 5–30 depending on the mineralogy, but the total range in $D'_A\delta$ is only slightly more than an order of magnitude for as wide a range of water contents as expected for most crustal conditions.

R. A. Yund
Department of Geological Sciences,
Brown University,
Providence, RI 02912, USA

Editorial responsibility: K. Hodges

Introduction

Transport rates along grain and inter-phase boundaries in rocks are poorly understood compared to volume diffusion rates in minerals because the former depend on the micro-structure of the aggregate and the nature of the boundaries, both of which are difficult to characterize. Grain boundary diffusion data prior to about 1990 were limited and summarized by Joesten (1991). Recent experimental studies using natural and synthetic polycrystalline aggregates (mostly monomineralic) have employed isotopic tracers and depth profiling or step scanning from the surface with an ion microprobe (SIMS) (Farver and Yund 1991b, 1992, 1995a), or used growth rates of reaction rims between incompatible phases (Brady. 1983; Yund and Tullis 1992; Fisler and Mackwell 1994). Both techniques provide experimental data for the product of the grain boundary diffusion coefficient (D') and the effective width of the grain boundary (δ), although the ion probe method can be used to determine D' independently of δ for a limited range of experimental conditions. Recent studies indicate that grain boundary widths are typically on the order of 1–3 nm, at least for essentially dry, unaltered mineral aggregates (e.g., Joesten 1991 and Farver et al. 1994).

The ion probe technique is especially useful for determining grain boundary diffusion co-efficients because data can be obtained over a range of temperatures and pressures, and the microstructure of the aggregate can be controlled by first equilibrating a sample with fluids which form different interfacial angles (Θ) with the minerals (Farver and Yund 1992). Like the rim method, the ion probe technique provides an average diffusivity for many grains but has two disadvantages: (1)

a knowledge of the volume diffusion rates for the isotope being studied is required; (2) the grain size of the aggregate typically must be $< \sim$ 10 μm in order to obtain sufficient isotopic signal (most of the analyzed volume is un-ex-changed original grains) and to minimize thermal cracking during heating and cooling. The difficulty of obtaining natural, very fine grained aggregates requires that low porosity, synthetic aggregates must be prepared for most minerals. Thermal cracking can occur during preparation of an aggregate or at the beginning or end of a diffusion experiment, making it difficult ot determine when cracking occurred and the effect, if any, on the resulting isotopic profiles. A technique has been developed to introduce the tracer at pressure and temperature and this eliminates most of this uncertainty (Farver and Yund 1995a). However, this technique does not eliminate the uncertainty which is introduced by grain growth during the diffusion anneal.

The growth rate of a polycrystalline reaction rim between two incompatible phases has been used for diffusion studies in several silicate aggregates (e.g., Brady 1983; Yund and Tullis 1992; Fisler and Mackwell 1994). The rim method avoids the problems associated with thermal cracking and grain growth, and it does not require hot-pressing of fine-grained starting materials or a knowledge of volume diffusion rates. The disadvantages are: (1) depending on the reaction, several atomic species may be involved in the transport including coupled diffusion of cations and oxygen or counter-interdiffusion of cations to maintain chemical and charge balance; (2) accurate measurements require relatively thick rims (typically $>$ 5–10 μm) and these long diffusion distances limit experiments to relatively high temperatures.

The goal of this study was to evaluate the effect of small differences in water concentration on grain boundary diffusion rates and to determine whether the microstructure of the rim was dependent on the experimental conditions of its growth. Most of the experiments were done using the reaction of olivine (Fo_{92}) plus quartz to produce enstatite rims. Some experiments were done with MgO plus synthetic $Mg_2Si_2O_6$ or MgO plus quartz; both pairs react to form forsterite rims. The ion probe method provides diffusion data for individual ions (isotopes) whereas two or more ions are involved in oxide/silicate rim studies. Therefore the results from the two methods cannot directly be compared, but data from both could provide important information about grain boundary diffusion rates for geological processes involving chemical changes. The rim method offers a convenient way to determine the effect of parameters such as confining pressure and water on diffusion rates. In as much as the rim growth and ion probe methods involve very different assumptions and approximations, a consistent set of data from the two methods would help to establish the reliability of experimentally determined grain boundary diffusion data.

The growth rates of enstatite rims as a function of the water content of the aggregate are presented first and evaluate in terms of nucleation and grain growth rates, followed by an evaluation of the effects of confining pressure, temperature and rim mineralogy. The rim growth rates are then used to calculate grain boundary diffusion rates ($D'_A\delta$) and these are compared with previously published data.

Experimental procedures

Olivine was separated by hand from the Balsam Gap dunite, Jackson County, North Carolina, crushed, and the 125–200 μm diameter size fraction separated. An electron probe analysis gave a composition of $Fo_{92.2\pm0.2}$ with the following wt % oxides: CaO = 0.01±0.01, Na_2O = 0.03±0.01, MnO=0.09±0.05. A clear quartz crystal from Brazil was crushed and sieved to obtain the 10–30 μm fraction. About 40 mg of olivine and 60 mg of quartz were used for each enstatite rim growth experiment. Approximately 125–200 μm diameter fragments of 99.99 % MgO single crystals, obtained from Norton Co., together with 10–30 μm quartz or 1–5 μm synthetic enstatite, were used for the forsterite rim growth experiments. Reactants were sealed in a Pt tube (0.15 mm wall) and 0.1 to 5.0 wt % water added. In most of the experiments in which less than 5.0 wt % water was added, a piece of pure talc was used as the source of the water in order to improve the accuracy of adding a small but known amount of water. Talc breaks down above ~ 820°C to water, enstatite, and quartz at the pressure of these experiments (e.g., Evans and Guggenheim 1988). Pure water was added instead of talc to some samples with identical results. For other experiments the starting materials were air dried at 150°C for 12 hours, or vacuum dried at 250°C for 8 hours, before quickly crimping and welding the last crimp on the Pt tube.

Experiments were done in a piston-cylinder apparatus with the Pt tube surrounded by either 3 mm of graphite or pyophyllite. Pyrophyllite or talc pieces outside the fumace were used for all experiments and a pressure correction of 30 % applied. This correction was based on calibration experiments at ~ 700 MPa using the forsterite/spinel transformation in Mg_2GeO_4. This equilibrium is known from phase equilibria and calorimetry data (e.g., Ross and Navrotsky 1987).

In order to measure rim growth rates accurately it is common to use large, flat sided single crystals which are surrounded by a fine-grained second phase and sectioned after the experiment. This procedure was not followed here because it would have been difficult to avoid crushing the single crystal during pressurization and to ensure essentially zero porosity near the single crystal interface. Therefore the errors in rim thicknesses in the experiments described here are somewhat larger than when single crystals are used. The rim thicknesses were determined optically using ~ 20 μm thick thin sections. Several measurements were made and averaged, taking care to measure only vertical and planar boundaries. Ion-thinned sections were made of some sample and examined by transmission electron microscopy (TEM) with a Philips 420T. Ortho-enstatite was identified from its electron diffraction pattern and twinning in these grains is common. The range of experimental conditions was from 250–700 MPa at 1000°C and from 950–1100°C at 700 MPa. At these conditions ortho-enstatite is the stable polymorphy (Carlson and Lindsley 1988), but for simplicity it will be referred to as enstatite in the following discussion.

Some samples were etched in HF vapor for several minutes, or for one hour in NH_4HF_2 (Wegner and Christie 1985), in order to make it easier to determine the grain size of the polycrystalline enstatite rims using an Hitachi Model S-2700 scanning electron microscope (SEM). Generally the NH_4HF_2 was more successful for etching the enstatite grain boundaries without destroying the olivine or quartz on either side of the rim.

Growth of enstatite rims between olivine and quartz

The thickness squared (X^2) of enstatite rims as a function of annealing time (t) is plotted on the following figures, where t is the duration of the experiment at the specified conditions. Such plots should yield a straight line if the growth rate is diffusion controlled (e.g., Fisher 1978). Growth rates or slopes of these curves are used in a later section to evaluate diffusion rates through the rims, but for now these plots are used to compare relative rim growth rates at various experimental conditions, and qualitatively to evaluate the nucleation rates as indicated by the intercepts on the time axis.

Effect of water content and pressure medium

Most experiments were done with Pt tubes (0.15 mm wall) which were embedded in graphite. The results for 700 MPa and 1000°C with 0.1 wt % water (talc) added are shown by the solid squares (lower line) on Fig. 1a. Similar experiments but with soft-fired pyrophyllite around the sample tube gave results shown by the crosses (upper line) on the figure. Clearly there is a difference in the slopes and probably in the intercepts for these two data sets. These samples contained so little water that it was not possible to confirm its presence (or loss) by weight difference before and after an experiment. On the basis of data presented below, it is believed that the difference in the two data sets shown in Fig. 1a is due to the loss of some (more) water from samples in the graphite assembly. The water content of the graphite around the Pt would be less than that of pyrophyllite undergoing dehydration, hence the graphite assemblies would produce a larger water or hydrogen gradient across the Pt tube. Diffusion of hydrogen through the tube would result in a decrease in the water fugacity of samples in graphite and this could be significant for samples with low (0.1 wt %) water contents. These

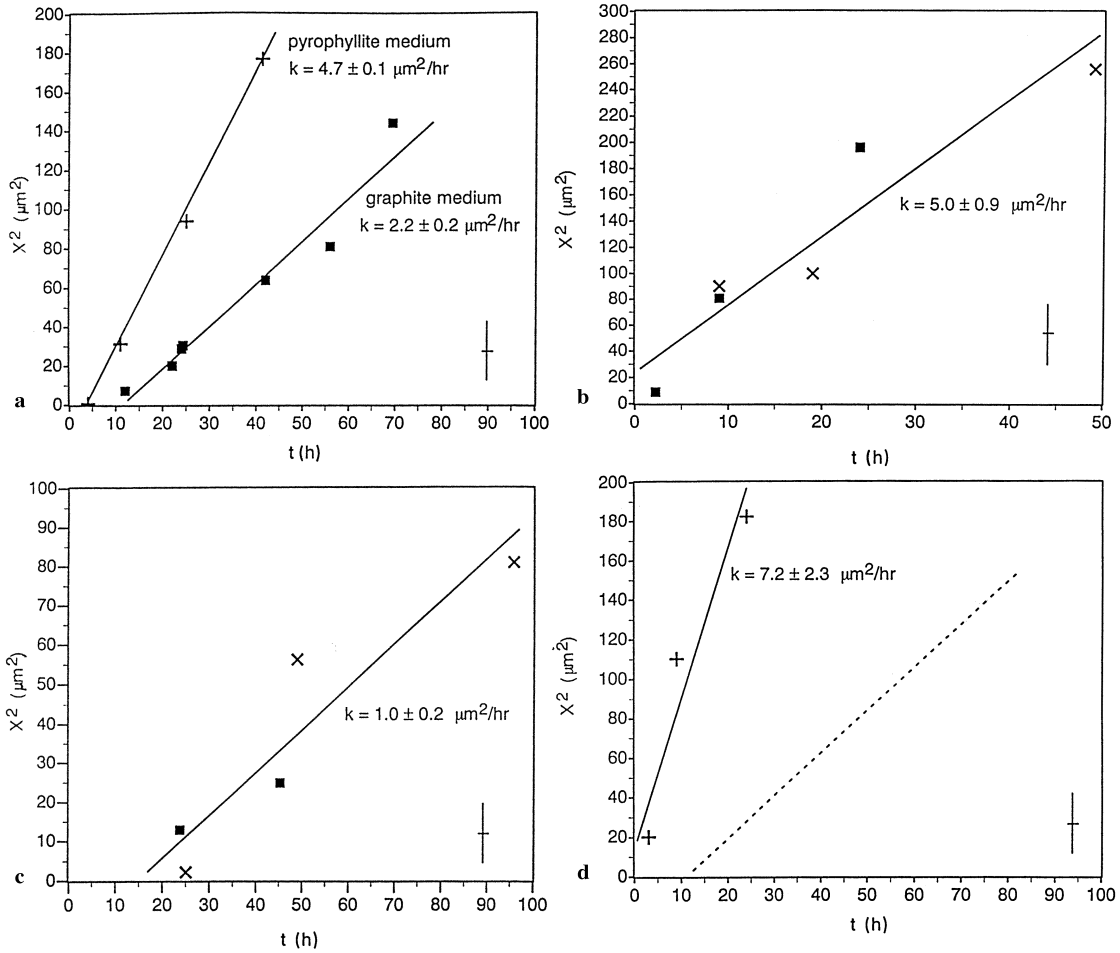

Fig. 1 a–d Enstatite rim thickness squared (X^2) versus time (t) for samples annealed at 1000°C and 700 MPa. All experiments in a graphite medium except as noted. Symbol in the *lower right-hand corner* represents a typical error bar for a 10 μm rim. Least squares calculated slopes (k) are shown. **a** Samples with 0.1 wt % water added using a graphtie (*solid squares-lower line*) or a pyrophyllite (*crosses - upper line*) pressure medium. There are two data points at ~24 hours in the lower data set. **b** Experiments with 1.0(X) or 5.0 (*solid squares*) wt % water added. **c** Samples first air dried at 150°C (*crosses*) or vacuum dried at 250°C (*solid squares*). **d** Experiments at 1400 MPa with 0.1 wt % water added. The *dashed line* is from **a**

observations and interpretation are consistent with conclusion by other researchers about loss of water in piston-cylinder experiments for different confining media (Douce and Beard 1994).

If hydrogen is lost from Pt tubes in the graphite assembly, one might expect to see a change in the growth rate at longer growth times. The fact that no change of slope is apparent in these or other experiments may be due to : (1) uncertainties in the data (possible); (2) water loss mostly occurring early in the experiment (unlikely); or (3) the growth rate being insensitive to the water loss as long as a trace amount of water remains (likely). Farver et al. (1994) have recently shown that an increase in the water fugacity from essentially zero to less than a bar increases Mg grain boundary diffusion rates in forsterite aggregates by about factor of five. Experiments in graphite at 700 MPa, 1000°C, with 1 and 5 wt % water are shown in Fig. 1b. (The presence of water at the end of these experiments was confirmed by weight loss after the tubes were opened and dried.) Within the uncertainty of the data, there is no difference in growth rate for samples with 1 and 5 wt % water. The slope for these experiments is greater (5.0±0.9 $\mu m^2/h$) than that for samples with 0.1 wt % water run in graphite assemblies (2.2±0.2 $\mu m^2/h$) but essentially identical to the slope for samples with 0.1 wt % water run in pyrophylite assemblies (4.7±0.1 $\mu m^2/h$).

The presence of water up to a certain amount enhances the nucleation rate as shown by the intercepts on the abscissa of Fig. 1a–c. Enstatite rims on samples with 1.0 or 5.0 wt % water have a more variable rim thickness and the interface with quartz tends to be less smooth compared to samples with < 1 wt % water, and these factors resulted in more scatter of the data. The details of the microstructures of these enstatite rims are presented below. A straight line has been fitted by least squares regression to all of the data in Fig. 1 and in subsequent plots.

Two buffered experiments were done with the Fo_{92} + quartz sealed in a Pt tube with 0.1 wt % water and this tube sealed inside a 0.2 mm thick Au tube with either the quartz + fayalite + magnetite (QFM) buffer (log fo_2 = −11.7 MPa), or the wustite + magnetite (WM) buffer (log fo_2 = 13.1 MPa), plus water (e.g., Huebner 1971). (All fo_2 are for 1000°C and 700 MPa.) These experiments were done in a graphite assembly and served two purposes: (1) the water remained in the outer tube and prevented loss of the small amount of water in the inner tube containing the sample; (2) the oxygen fugacity was controlled and insured that the olivine was stable. Water was observed in the outer Au tube at the end of these experiments for 25.0 h at 1000°C and 700 MPa. According to the data of Nitsan (1974), Fo_{92} is stable between the Ni + NiO buffer (log fo_2 = ~ −11.0 MPa) and the quartz + fayalite + Fe butter (log fo_2 = ~ −16.3), and no evidence of olivine breakdown was observed in these experiments by TEM.

The rim thickness in the QFM buffered sample was 8.1±1.0 μm compared to 7.8±1.0 μm for the WM buffered sample. At the same conditions the value for an unbuffered sample in a pyrophyllite assembly was 9.6±1.0 μm and an unbuffered sample in a graphite assembly was 5.0±1.0 μm. The rim thicknesses for the buffered any pyrophyllite experiments are the same within experimental error, indicating that any water loss from samples in pyrophyllite assemblies was to small to be significant for rim growth rate. The smaller rim thickness for the unbuffered graphite experiment is consistent with it having lost some water. For experiments using a graphite assembly, the log fo_2 is effectively buffered at ~ −13.5 MPa, well within the olivine stability field and consistent with the observation that olivine was stable in these experiments.

Additional experiments were done with carefully dried samples to evaluate further the importance of a small amount of water on nucleation and growth rates of enstatite rims. Rim growth in samples initially air dried at 150°C and others vacumm dried at 250°C before sealing are shown in Fig. 1c. Within the uncertainties there is no difference in the results for these two different drying procedures, but the slope is significantly lower (1.0±0.2 $\mu m^2/h$), and the intercept larger, than for the water-added experiments (5.0±0.2 $\mu m^2/h$). This indicates that both nucleation and growth rates are faster in the presence of a small amount of water, but there is little if any change in growth rates when more than ~0.1 wt % water is present. This observation is significant for interpreting grain boundary diffusion rates in a later section.

Microstructure of rims

The rims in the above experiments consist of fine-grained enstatite; representative optical, TEM, and SEM micrographs are shown in Fig. 2. The mean linear intercept lengths of these enstatite grains were determined from SEM micrographs and are reported below without applying a factor, usually between 1.2 and 1.9 (Gifkins 1970), to convert these intercept lengths to grain diameters.

The rims in the 0.1 wt % water-added experiments are composed of enstatite grains which tend to form an equilibrium microstructure consisting of triple junctions with 120°angles (Figs. 2d and f). The mean linear intercept length increases from 0.9±0.1 μm to 1.4±0.2 μm between 12.0 h (rim thickness = 2.7 μm) and 22.0 h (rim thickness = 4.5 μm). Grain growth decreases after this and the intercept length is only 1.6±0.2 μm after 56.0 h (rim thickness = 9.0 μm). Compare Fig. 2d and e. Therefore, for most of the data represented by the lower line on Fig. 1a, there is a change in grain diameter of less than a factor of two. Grain growth rates for samples with 0.1 wt % water added run in pyrophyllite assemblies are the same as those done in graphite assemblies within experimental error. There is little if any evidence for a decrease in slopes of the lines in Fig. 1 which could be attributed to grain growth during rim formation.

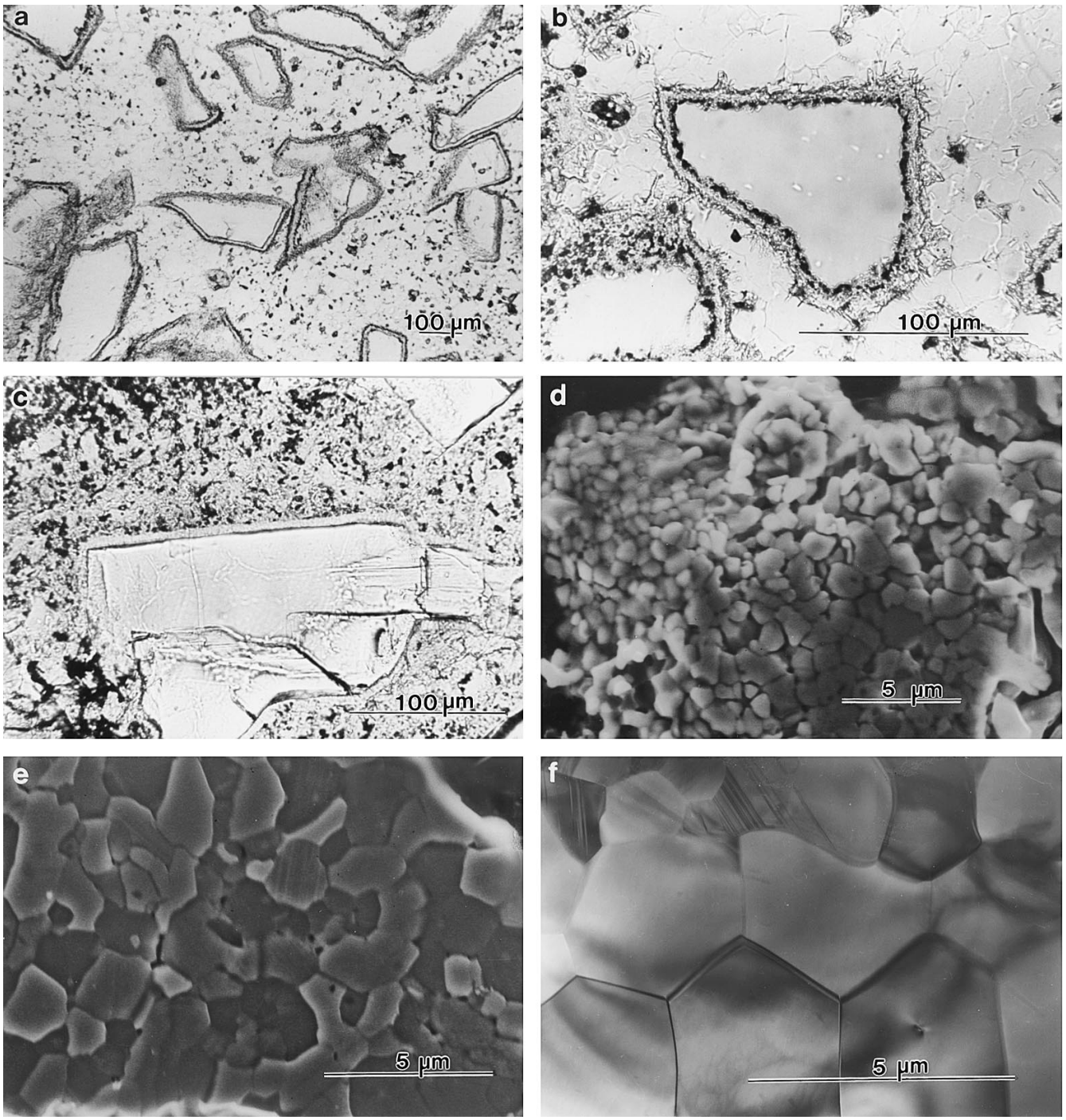

Fig. 2 a–f Micrographs of reaction rims formed at 700 MPa and 1000°C. **a** Optical micrograph of En rims around Fo_{92} grains in a Qtz matrix with 0.1 wt % water added after 92 h. **b** Similar to **a** but with 1.0 wt % water added and after 25 h. Note irregular interface between En and Qtz and the concentration of iron oxides near the Fo-En interface. **c** Optical micrograph of Fo_{100} rims between MgO and fine-grained En after 68 h. Sample initially vacuum dried at 250°C for 8 h. **d** SEM micrograph of En grains in a rim formed after 12 h with 0.1 wt % water added. **e** Similar to **d** but after 22 h. Shorter etching time than previous micrograph. **f** TEM micrograph of En grains in a sample with 0.1 wt % water added after 51 h. Note twinned En grains in upper portion of micrograph

Compared to the data for samples with 0.1 wt % water added, enstatite grain growth is faster in the samples with 1.0 wt % water added. The mean linear intercept length is 1.0±0.1 μm after 2.2 h (3.0 μm rim) and reaches 2.1±0.3 μm after 9.0 h (9.6 μm rim). Although there is some reduction in the rate of grain growth at longer times, after 25.0 h the mean intercept length is 3.3±0.5 μm which is about twice that for a similar sample with 0.1 wt % water added. There is a larger range in grain size in the longer experiments with

1.0 wt % water. After 25 h a sample with 5.0 wt % water (rim thickness = 10.0 μm) had a mean intercept length of 2.7±0.3 μm, which is no larger than that in a sample with 1.0 wt % water. There was no evidence of an increase in porosity in the samples with a higher water content, and no evidence of interconnected channels as a result of a dihedral angle < 60°.Grains of iron oxides (~ 0.5 μm diameter) precipitated in the enstatite rim and were mostly FeO, although some grains may have been Fe_3O_4; see Fig. 2b. Energy dispersive analysis of the enstatite grains indicated that they contain < 1 mol % of the ferrosilite component.

Examination of enstatite and forsterite rims by TEM indicated that the grain boundaries have essentially no observable porosity and all boundaries imaged in diffuse dark-field are <~ 10 nm wide. (Lattice fringes were not imaged for grain boundaries because the narrow enstatite rims were rarely well thinned and a few such images may not be representative of the aggregate.) The presence of tight grain boundaries is not unexpected because the enstatite nucleated and grew at 700 MPa. Any porosity at or near the olivine/quartz interface was eliminated by grain growth and some recrystallization of the quartz within the first few hours of these experiments.

Effect of confining pressure and temperature

Three experiments were done at 1400 MPa and 1000°C in graphite assemblies with 0.1 wt % water added to determine whether a higher confining pressure had a significant effect on the enstatite rim growth rate. Although the dependence of D'δ on confining pressure was expected to be minor (e.g., Farver et al. 1994), the porosity or microstructure of the rim might change with pressure and affect the rim growth rate. The results are shown in Fig. 1d and include the line for the 700 MPa data (graphite assembly) from Fig. 1a for comparison. The 1400 MPa data have a steeper slope (7.2±2.3 μm^2/h) than those for experiments at 700 MPa (2.2±0.2 μm^2/h) in graphite, but about the same slope (4.7±0.1 μm^2/h) within experimental error as for the 700 MPa experiments in pyrophyllite. The similarity with the 700 MPa experiments done in pyrophyllite suggests that for experiments done in graphite, water may have been lost more slowly from the 1400 MPa samples. This interpretation is consistent with the lower intercept of the higher pressure data on the abscissa, indicating that enstatite nucleation was easier. There is no evidence that the rim growth rate, and hence either D' or δ, is significantly affected by pressure in the range from 700 to 1400 MPa.

Experiments were also done at 580, 450, and 210 MPa at 1000°C in graphite assemblies with 1.0 wt % water added. The data are shown in Fig. 3a along with the 700 MPa data from Fig. 1b for comparison. The rim thickness is less at 580 and 450 MPa than at 700 MPa for the same time. Three experiments at 450 MPa indicate,

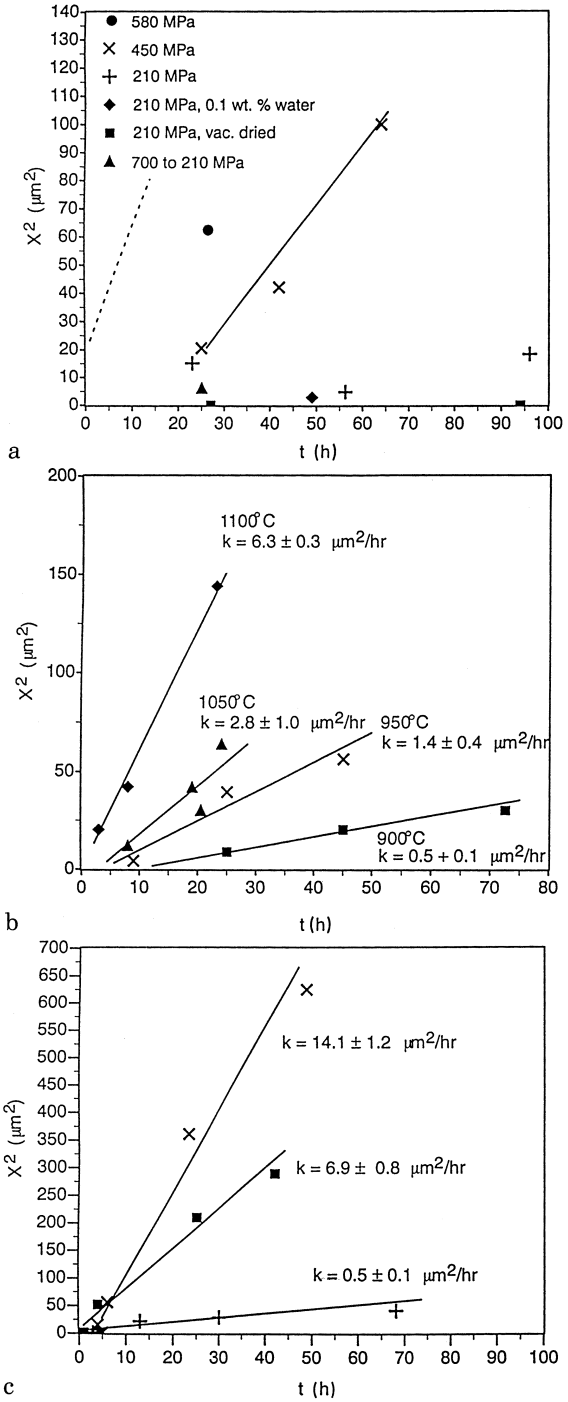

Fig. 3a Effect of confining pressure <700 MPa on enstatie rim growth in graphite assemblies at 1000°C. All samples had 1.0 wt % water added except for one sample with 0.1 wt % water (*solid diamond*) and two sample (*solid squares*) on the abscissa which were vacuum dried at 250°C. The sample shown by the *solid triangle* was first annealed at 700 MPa for 22 h, then annealed at 210 MPa for 228 h. The *solid line* is drawn through the 450 MPa data (*crosses*); the *dashed line* is from Fig. 1a (graphite). **b** Tempeature dependence of enstatite rim growth at 700 MPa with 0.1 wt % water added (graphite assembly). **c** Growth rate of forsterite rims at 1000°C and 700 MPa in graphite. The five *xs*(*upper line*)are for samples with 0.1 wt % water added and the five *crosses* (*lowest line*) are for samples vacuum dried at 250°C for 80 h; both data sets are for the reaction $Mg_2Si_2O_6 + 2MgO = 2Mg_2SiO_4$. The four *solid squares* are for the reaction $2MgO + SiO_2 = Mg_2SiO_4$ and had 0.1 wt % water added

however, that the line through these data is approximately parallel to that for the 700 MPa data although it has a larger intercept on the time axis. Thus it appears that the growth rates are very similar at 450 and 700 MPa, but nucleation of enstatite is more difficult at lower pressure. The water contents of all these samples were the same, but at lower confining pressure the fugacity of water was lower, although unknown, because the samples were not saturated with water.

Three experiments at 210 MPa indicate that the rim thickness is even less for a given annealing time at this low pressure. Although some nucleation occurred, the lack of continued growth does not necessarily reflect a decreases in the growth rate because thickening of the rim appears to involve continued nucleation of enstatite. Although continued nucleation would occur on early formed enstatite grains, the two new interfaces (olivine/enstatite and enstatite/quartz) would be closer to local equilibrium than the initial quartz/olivine interface and the local Gibbs energy difference for continued nucleation at these interfaces would be less.

The difficulty of nucleating or growing enstatite rims in samples with low or no water and at 210 MPa is shown by an experiment with 0.1 wt % water (diamond on Fig. 3a), and two experiments with vacuum-dried samples (solid squares on abscissa of Fig. 3a). Together the data in Fig. 3a strongly suggest that the formation of enstatite rims is controlled by the nucleation rate when the water fugacity is low. Thus determination of diffusion rates from rim growth rates must be done with caution for this and other reactions when nucleation is slow.

There is a narrow temperature range that can be used to study enstatite rim growth rates, as well as most rim growth rates when water is present, because the chemical flux through a several micron thick rim is slow and the rim has to at least double in thickness on a laboratory time scale in order that the growth rate can accurately be determined. Data for enstatite growth rates were obtained between 900 and 1100°C at 50°C intervals and are shown in Fig. 3b. All of these experiments were done with 0.1 wt % water added at a confining pressure of 700 MPa. As expected, the growth rate decreases with decreasing temperature; these data will be used in a later section to estimate an approximate activation energy for grain boundary diffusion.

Forsterite rim formation

The growth rates of reaction rims between large fragments of MgO crystals and fine-grained, synthetic enstatite in graphite assemblies at 1000°C and 700 MPa are shown in Fig. 3c. There is a significant difference between the growth rates for samples with 0.1 wt % water added (upper line on Fig. 3c) and those vacuum dried at 250°C for 8 h before sealing (lower line). This observation is consistent with the results for enstatite rim growth although the growth rate of forsterite rims with 0.1 wt % water appears to be slightly faster than that for enstatite rims at the same conditions (compare Figs. 3c and 1a). The growth rate for forsterite rims in the vacuum-dried samples is significantly slower than that for enstatite rims at the same conditions (compare Figs. 3c and 1c).

The line for forsterite rims in the 0.1 wt % water-added samples passes approximately though the origin, indicating that nucleation of forsterite is relatively rapid compared to its growth rate. The data for the vacuum-dried samples also have an intercept near the origin indicating that the nucleation rate is not very different for forsterite in vacuum-dried and water-added samples. For comparison, a second set of experiments was done using the reaction $2MgO + SiO_2 = Mg_2SiO_4$ with 0.1 wt % water added (solid squares in Fig. 3c). Local equilibrium requires a rim of enstatite between forsterite and quartz, but only forsterite formed in these experiments because of the slow nucleation of enstatite at these conditions (see also Brady, 1983).

The TEM observations of some of these forsterite rims indicated that the rims have no visible porosity and the forsterite grains have about the same size as the enstatite grains described above. An optical micrograph of a forsterite rim grown for 68 h in a vacuum-dried sample is shown in Fig. 2c. The width of these as well as the enstatite rims, was very uniform in dried samples. No attempt was made to evaluate grain growth of forsterite because preliminary observations indicated forsterite grain growth was not significant in terms of evaluating diffusion rates through the rims.

Grain boundary diffusion rates

The product of the grain boundary diffusion coefficient (D') times the effective grain boundary width (δ) can be obtained from rim growth rates for a reaction which is dominated by the diffusion of one component. The relation between D'δ and rim growth rate has been discussed numerous times (e.g., Brindley and Hayami 1965; Shatynski et al. 1976; Brady 1983; Walther and Wood 1984; Watson 1986; Rubie 1986; Fisler and Mackwell 1994). The following is based on a formulation given by Fisher (1978) for growth of a plane layer interface, which is applicable to our experimental results.

Determination of diffusion rates from rim growth rates

The reaction $\alpha A + B = A_\alpha B$ will be symbolized as $A|A_\alpha B|B$ and the growth of the layer or rim $A_\alpha B$ is parabolic if growth is diffusion controlled. Following the notation in Fisher (1978), the thickness of the layer (X_ϕ) is given by:

$$X_\phi^2 = 2k_p^\phi t \ , \qquad (1)$$

where k_p^ϕ is the parabolic rate constant which is a function of concentration, the driving force for the reaction,

the diffusion coefficent, and a scaling distance. Fisher (1978) derived the following expression for k_p^{ϕ} for growth of a layer controlled by diffusion of a single component, A:

$$k_p^{\phi}\left[\sum(v_\phi/v_A)\right]L_{AA}V_\phi\Delta\mu_A \ , \tag{2}$$

where $\sum(v_\phi/v_A)$ includes the stoichiometric coefficient of the product phase (s) (v_ϕ) and the stoichiometric coefficient of the diffusing component (v_A) forming the layer. This term is equivalent to the stoichiometric coefficient (ζ) of Schmalzried (1978), which he defined as the number of moles of rim phase(s) produced for each mole of diffusing component. Term L_{AA} is the phenomenological diffusion coefficient and $\Delta\mu_A$ is the difference in the chemical potential of A across the layer. The following standard expression can be substituted for L_{AA}

$$L_{AA} = c_A D_A/RT \ , \tag{3}$$

where c_A is the concentration of A in the layer, D_A is the effective diffusion coefficient for A, and R and T have their usual meanings. Assuming grain boundary diffusion of A (D'_A) is rate controlling, the following expression can be substituted for D_A when the grain diameter is small (Joesten 1991):

$$D_A = \pi\sigma D'_A/2d, \tag{4}$$

where σ is the grain boundary width and d is the mean diameter of grains in the product layer. Combining Eqs. (2), (3), and (4) gives:

$$k_p^{\phi} = \left[\sum(v_\phi/v_A)\right]c_A\ V_\phi\ \pi\ \delta\ D_A\ \Delta\mu_A/2dRT \ , \tag{5}$$

and

$$X_\phi^2 = \left[\sum(v_\phi/v_A)\right]c_A\ V_\phi\ \pi\ \delta\ D_A\ \Delta\mu_A t\ /\ 2dRT \ , \tag{6}$$

Solving for $D'_A\delta$ in (6):

$$D'_A\delta = d\ RT\ X_\phi^2/\left(\pi\left[\sum(v_\phi/v_A)\right]c_A V_\phi\Delta\mu_A t\right) \ . \tag{7}$$

For the reaction $SiO_2 + 2MgO = Mg_2SiO_4$ and assuming MgO is the diffusing component, the value of $\sum(v_\phi/v_{MgO}) = -1/2$ and Eq. (7) becomes:

$$D'_{MgO}\delta = -2\ d\ RT\ X_{Fo}^2/(\pi\ c_{MgO}V_{Fo}V_{Fo}\ \Delta\mu_{MgO}t) \ . \tag{8}$$

Equation (7) is similar to the expression for D'_A given by Fisler and Mackwell (1994) which they used to analyze diffusion through a fayalite rim produced by the reaction $2FeO + SiO_2 = Fe_2SiO_4$. Ray Joesten (personal communication and manuscript in preparation) has pointed out that for a reaction between oxide phases such as $SiO_2 + 2MgO = Mg_2SiO_4$, one can obtain only values for D'_{MgO}, D'_{SiO_2}, or D'_{Mg_2Si-1}; values for the diffusivites of individual ions can not be extracted from rim growth rate data. We will return to this problem in the section below.

For the reaction $SiO_2 + Mg_2SiO_4 = Mg_2Si_2O_6$, the difference in chemical potential of SiO_2 ($\Delta\mu_{SiO_2}^{Q|En|Fo}$) is related to the Gibbs energy (G) of the phases (calculated from data of Holland and Powell, 1990):

$$\begin{aligned}\Delta\mu_{SiO_2}^{Q|En|Fo} &= \mu_{SiO_2}^{Q|En} - \mu_{SiO_2}^{En|FO}\\ &= (G_Q + G_{Fo}) - G\text{En} - G_{En}\\ &= -\Delta G_R = 8.4\text{kJ/mole at } 1000^\circ C \ .\end{aligned}$$

Similarly for MgO:

$$\begin{aligned}\Delta\mu_{MgO}^{Q|En|Fo} &= \mu_{MgO}^{Q|En} - \mu_{MgO}^{En|Fo}\\ &= G_{En} - (G_{Fo} + G_Q)\\ &= \Delta G_R = -8.4\ \text{kJ/mole} \ .\end{aligned}$$

Rim growth may also involve the interdiffusion of Mg and Si and the difference in chemical potential for the component Mg_2Si_{-1} is given by:

$$\begin{aligned}\Delta\mu_{Mg_2Si_{-1}}^{Q|En|Fo} &= \mu_{MgO_2Si_{-1}}^{Q|En} - \mu_{Mg_2Si_{-1}}^{En|Fo}\\ &= 3G_{En} - 3(G_{Fo} + G_Q) = 3\Delta G_R\\ &= -25.2\ ;\text{kJ/mole} \ .\end{aligned}$$

Similar expressions can be written for $\Delta\mu_A$ of the other possible diffusing components in the two additional rim reactions (En|Fo|per and Q|Fo|Per) investigated in this study. The values for $\Delta\mu_{SiO_2}^{Q|En|Fo}$, $\Delta\mu_{MgO}^{En|Fo|Per}$, $\Delta\mu_{Mg_2Si_{-1}}^{En|Fo|Per}$, $\Delta\mu_{SiO_2}^{Q|Fo|Per}$, $\Delta\mu_{MgO}^{Q|Fo|Per}$, and $\Delta\mu_{Mg_2Si_{-1}}^{Q|Fo|Per}$ are given in Table 1.

Identification of the diffusing component

An inert marker, such as a Pt wire, has been used to identify the diffusing component during rim growth by observing which side of the inert marker the product phase grows on (e.g., Brindley and Hayami 1965). This technique is not very sensitive and although we tried such experiments we cannot identify whether the diffusing component involved an oxide, either MgO or SiO_2, or whether it was Mg_2Si_{-1}; the interdiffusion of Mg and Si. In the following discussion we will calculate diffusion coefficients for each of these three possible components assuming in turn that each is rate controlling. Thus the three values cannot be compared to each other because each is calculated assuming it is rate controlling. Even if the diffusing component is known, two or more ions are involved. Consequently a direct comparison cannot be made with $D'\delta$ values for individual ions obtained from isotopic profiles determined using an ion microprobe. Furthermore it should be noted that even if the diffusing components is known, the identities of the actual chemical specie(s) which migrate along a grain boundary are not known; the migrating species could be individual ions, oxides, hydrated ions, or more complex chemical species. For example, due to size consideration it seems unlikely that Mg and O diffuse as molecular MgO, although because MgO is electrically neutral it might be less attracted to the charged interfaces of a grain boundary.

Table 1 Values used to calculate $D'_{SiO_2}\delta$, $D'_{MgO}\delta$ and $D'_{Mg_2Si-1}\delta$ from Eq. (7) for 1000°C and 700 Mpa. Values for $\Delta\mu_A$ are kJ/mole and calculated from the data in Holland and Powell (1990). (*Fo* forsterite, *En* enstatite, *Per* periclase *Qtz* quartz)

	Fo + Qtz = En	En+2Per = 2Fo	2Per + Qtz = Fo
$\sum(v_\phi/v_{SiO_2}$	1	2	1
$\sum(v_\phi/v_{MgO})$	− 1	− 1	− 1/2
$\sum(v_\phi/v_{Mg_2Si-1})$	− 3	− 4	− 2
C_{SiO_2}	$2/V_\phi$	$1/V_\phi$	$1/V_\phi$
C_{MgO}	$2/V_\phi$	$2/V_\phi$	$2/V_\phi$
C_{Mg_2Si-1}	$1/V_\phi$	$1/V_\phi$	$1/V_\phi$
$\Delta\mu_{SiO_2}$	8.4	48.6	57.0
$\Delta\mu_{MgO}$	− 8.4	− 24.3	− 28.5
$\Delta\mu_{Mg_2Si-1}$	− 25.2	− 97.3	− 114.0

Grain boundary diffusion rates in enstatite and forsterite aggregates

For comparison between experiments involving the same reaction at different conditions, the uncertainty in $D'_A\delta$, where A = MgO, SiO_2, or Mg_2Si_{-1}, is primarily determined by the error in the experimental growth rate. This uncertainty is < 2 and similar to the reproducibility of $D'_A\delta$ values obtained from ion probe diffusion profiles. The absolute error in $D'_A\delta$ is larger and includes the uncertainties in all the parameters. This error is estimated to be $\pm$ 3 to 4 times the reported values.

The values for $D'_{SiO_2}\delta$, $D'_{MgO}\delta$, $D'_{Mg_2Si-1}\delta$ are listed in Table 2 and values for $D'_{SiO_2}\delta$ are shown on the Arrhenius plot in Fig. 4. For the two rim reactions which produced forsterite, the difference in $D'_A\delta$ values is about a factor of eight; for the reaction which produced enstatite the difference in $D'_A\delta$ is less than five. The effects of confining pressure, temperature, and mineralogy on $D'_A\delta$ are discussed first, then the dependence of $D'_A\delta$ on water content is considered. These effects are arbitrarily discussed with reference to $D'_{SiO_2}\delta$; $D'_{MgO}\delta$ and $D'_{Mg_2Si-1}\delta$ show the same dependence on these parameters for a given reaction.

Effect of pressure

Pressure between 450 and 1400 MPa has a minor effect on the diffusion rate across enstatite rims for experiments with the same water content. The difference is less than the uncertainty in $D_{SiO_2}\delta$. This difference in $D_{SiO_2}\delta$ is consistent with the small activation volume of ~1.0cm^3 reported for ^{26}Mg grain boundary diffusion in forsterite aggregates using the ion microprobe technique (Farver et al. 1994). Together the available but limited data indicate there is not a large effect of pressure on grain boundary diffusion at crustal conditions. A relatively minor effect of confining pressure at crustal conditions on volume diffusion rates for silicates has been reported (e.g., Brady 1995).

The principal effect of pressure on these rim reactions is on the nucleation rate of enstatite, which appears to decrease with decreasing pressure (Fig. 3a). This makes determination of growth rates and hence diffusion rates more difficult at low pressure. In addition, when rim growth experiments are done at a few hundred MPa the microstructure or porosity of the rim may be critical. For example, Brady (1983) did a study using MgO single crystals surrounded by powdered quartz at 650–700°C

Table 2 $D'_A\delta$ (m^3/s) calculated from rim growth rates

Rim	Wt% H_2O	[a]k(μm^2/h)	$D'_{SiO_2}\delta$	$D'_{MgO}\delta$	$D'_{Mg_2Si-1}\delta$
[b]Enstatite	0.1 (Fig 1a)	4.7 ± 0.1	5.2×10^{-22}	$= D'_{SiO_2}\delta$	1.2×10^{-22}
Enstatite	0.1 (Fig 1a)	2.2 ± 0.2	2.5×10^{-22}	$= D'_{SiO_2}\delta$	5.5×10^{-23}
Enstatite	1–5 (Fig 1b)	5.0 ± 0.9	5.6×10^{-22}	$= D'_{SiO_2}\delta$	1.2×10^{-22}
Enstatite	Vacuum dried (Fig 1c)	1.0 ± 0.2	1.1×10^{-22}	$= D'_{SiO_2}\delta$	2.5×10^{-23}
[c]Enstatite	0.1 (Fig 1d)	7.2 ± 2.3	6.1×10^{-22}	$= D'_{SiO_2}\delta$	1.4×10^{-22}
[d]Enstatite	0.1 (Fig 3b)	0.5 ± 0.1	5.3×10^{-23}	$= D'_{SiO_2}\delta$	1.2×10^{-23}
[e]Enstatite	0.1 (Fig 3b)	1.4 ± 0.4	1.5×10^{-22}	$= D'_{SiO_2}\delta$	3.4×10^{-23}
[f]Enstatite	0.1 (Fig 3b)	2.8 ± 1.0	3.2×10^{-22}	$= D'_{SiO_2}\delta$	7.1×10^{-23}
[g]Enstatite	0.1 (Fig 3b)	6.3 ± 0.3	7.2×10^{-22}	$= D'_{SiO_2}\delta$	1.6×10^{-22}
Forsterite	0.1 (Fig 3c)	14.1 ± 1.2	2.7×10^{-22}	5.4×10^{-22}	6.8×10^{-23}
Forsterite	Vacuum dried (Fig 3c)	0.5 ± 0.1	9.6×10^{-24}	1.9×10^{-23}	2.4×10^{-24}
Forsterite	0.1 (Fig 3c)	6.9 ± 0.8	2.3×10^{-22}	4.5×10^{-22}	5.7×10^{-23}

[a] All at 1000°C and 700 MPa in graphite assembly except as noted. Growth rate (k) is from text figure indicated in parentheses
[b] Pyrophyllite assembly
[c] Pressure = 1400 MPa and $\Delta\mu_{SiO_2}$=11.1 kJ/mole, $\Delta\mu_{MgO}$=−11.1 kJ/mole, $\Delta\mu_{Mg_2Si-1} = -33.2$ kJ/mole. More water may have been retained than in experiments at lower pressure. See text
[d] T = 900°C: $\Delta\mu_{SiO_2} = 8.1$kJ/mole, $\Delta\mu_{MgO} = -8.1$ kJ/mole, $\Delta\mu_{Mg_2Si-1} = -24.2$kJ/mole
[e] T = 950°C: $\Delta\mu_{SiO_2} = 8.2$kJ/mole, $\Delta\mu_{MgO} = -8.2$ kJ/mole, $\Delta\mu_{Mg_2Si-1} = -24.6$kJ/mole
[f] T = 1050°C: $\Delta\mu_{SiO_2} = 8.6$kJ/mole, $\Delta\mu_{MgO} = -8.6$ kJ/mole, $\Delta\mu_{Mg_2Si-1} = -25.7$kJ/mole
[g] T = 1100°C: $\Delta\mu_{SiO_2} = 8.8$kJ/mole, $\Delta\mu_{MgO} = -8.8$ kJ/mole, $\Delta\mu_{Mg_2Si-1} = -26.3$kJ/mole

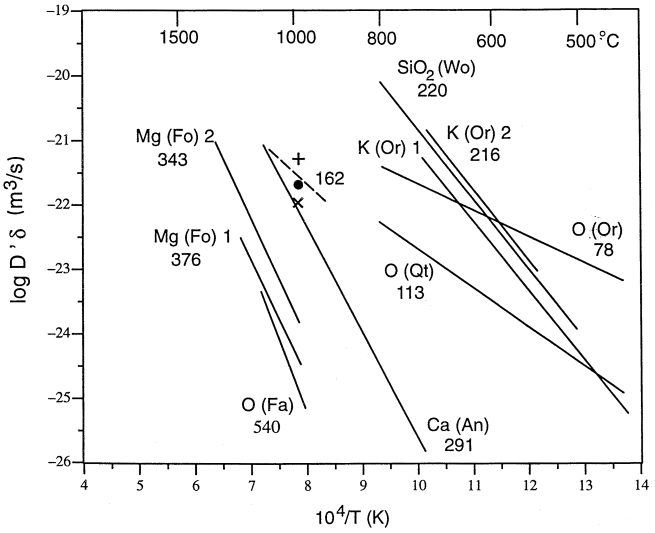

Fig. 4 Comparison of grain boundary diffusion data for silica in enstatite and forsterite rims from this study at 1000°C 700 MPa (+enstatite with 1–5 wt % water added and x samples vacuum dried at 250°C; • forsterite with ~ 0.1 wt % water added and ■ samples vacuum dried at 250°C). The *dashed line* shows the temperature dependence (162±30 kJ/mole) for enstatie rims with 0.1 wt % water added. The *solid lines* are from previous studies with activation energies in KJ/Mole give below the identification *laters: Mg*(*Fo*) is for ^{26}Mg in synthetic forsterite at 1 atm with gas mixtures of CO + CO_2 (*line 1*) and H_2 + CO_2 (*line 2*) (Farver et al. 1994); *O* (*Fa*) is oxygen in fayalite rims at 1 atm (Fisler and Mackwell 1994); *Ca*(*An*) is ^{42}Ca in synthetic anorthite at 1 atm, *K*(*Or*) is ^{41}K in synthetic orthoclase at 1 atm (*line 1*) and at 100 MPa P_{H_2O} (*line 2*) , *O*(*Or*) is ^{18}O in orthoclase at 100 MPa water pressure (Farver and Yund 1991); *SiO*$_2$(*Wo*) is SiO_2 in natural wollastonite rims (Joesten and Fisher 1988)

and 100 MPa water pressure. A forsterite rim about 20–30 μm thick formed initially around the MgO crystals but a further increase in thickness was not observed even after eight weeks. It is likely that forsterite nucleated over a wide zone because ions diffused rapidly through the interconnected aqueous fluid in the initially porous quartz aggregate. As the porosity of the rim decreased due to continued grain growth of forsterite, the flux of MgO or SiO_2 at these low temperatures essentially ceased through the thick, non-porous rim and further growth was not measurable.

Effect of temperature

The temperature dependence of diffusion through the enstatite rims is shown on the Arrhenisu plot of Fig. 4 by the dashed line; the data are listed in Table 2. This corresponds to an activation energy of 162 ± 30 kJ/mole. The large uncertainty is due to the limited number of experiments at each temperature (Fig. 3b) and the narrow temperature interval for which rim growth can be measured. (The ion probe method clearly offers an advantage over the rim growth method in terms of the number of experiments needed to determine accurately the activation energy for grain boundary diffusion.) Recognizing the large uncertainty, this activation energy is lower by a factor of ~2 to 3 than activation energies previously reported for grain boundary diffusion of oxygen and cations in forsterite and fayalite aggregates, and closer to the value for SiO_2 in natural wollastonite (220 kJ/mole) (Joesten and Fisher 1988) and for O in feldspar (78 kJ/mole) and quartz aggregates (113kJ/mole) at $P_{H_2O} = 100$. MPa (Farver and Yund 1995a). The activation energies shown on Fig. 4 do not appear to correlate with water content or water fugacity, the mineralogy of the aggregate, or the size or charge of the diffusing ions (assuming ions are the diffusing species).

Effect of rim mineralogy

The two sets of forsterite rim experiments (Fig. 3c) with 0.1 wt % water give the same value for $D'_{SiO_2}\delta$ within experimental error (Table 2). Furthermore, the values of $D'_{SiO_2}\delta$ for forsterite and enstatite with 0.1 wt % water are the same within experimental error. For vacuum-dried samples, $D'_{SiO_2}\delta$ for enstatite is about 17 times larger than that for forsterite, and the difference between vacuum-dried samples and those with 0.1 wt % water added is larger for the forsterite aggregates (Fig. 4). Similar comparisons can be made assuming MgO or Mg_2Si_{-1} is the diffusing component in these experiments.

Effect of water

The values for $D'_{SiO_2}\delta$ in the enstatite rims differ by a factor of ~ 5 between samples saturated with water (1–5 wt %) and those with a small but unknown amount of water after being vacuum dried at 250°C. There may be a factor of two difference in the diffusion rates for samples with ~ 0.1 wt % and those saturated with water. Vacuum drying at 250°C does not remove all of the absorbed water from quartz (Gee et al. 1990) and trace amounts of water may come from fluid inclusions in the starting materials, although Brazil quartz was chosen because it typically contains only tens of ppm of water (e.g., Kronenberg et al. 1986). The effect of water of $D'_{SiO_2}\delta$ is larger for forsterite rims; $D'_{SiO_2}\delta$ for samples with 0.1 wt % is ~ 28 times greater than that for similar samples which were first vacuum dried at 250°C.

The rate of ^{26}Mg grain boundary diffusion in synthetic forsterite aggregates increases from essentially water absent to water present conditions (Farver et al. 1994). They reported that this diffusion was about five times faster for samples annealed at one atmosphere in an H_2 + CO_2 gas mixture compared to those annealed in CO + CO_2, all at the same fo_2 (Fig. 4.). This difference was presumed to be related to a higher activity of water, or of a related species such as H^+, OH^-, or H_3O^+, in the H_2 + CO_2 gas mixture. The observed increase in $D'\delta$ for enstatite in this study is less than the increase in the diffusivity of ^{41}K in K-feldspar aggregates annealed at 1 atmosphere in air and at 100 MPa water pressure

(Farver and Yund 1995a) (Fig. 4). Together these data suggest that most of the enhancement in grain boundary diffusion rates occurs for water contents below about 0.1 wt % , and higher water contents or fugacities have a minor effect.

The range of water contents in the experiments reported here is likely to include the range in most metamorphic and igneous crustal rocks. The relatively minor effect of water on grain boundary diffusion rates observed in these and other experiments is in sharp contrast to an increase of several orders of magnitude of the Si and O volume diffusion rates in silicates for hydrothermal versus essentially dry samples. (See data summarized in Brady, 1993.) Oxygen volume diffusion rates in diffusion rates in feldspar and quartz correlate with water fugacity (Farver and Yund 1990, 1991a); and NaSi-CaAl interdiffusion rates in plagioclase are several orders of magnitude greater when "water" is present (Liu and Yund 1992).

The nature of water in a grain boundary and how it affects diffusion rates is problematical; water could be present as a thin film, similar to water adsorbed on a mineral surface (Parks 1990), it might occur as "isolated" molecules (a "hydrated" boundary), or it might create defects (Nowotny 1991). The properties and nature of a thin film of water (< few nm) depend on the nature of surface forces between atoms in the adjacent crystals and those in the aqueous fluid. These forces can be classified as "long range" or "short range" on the atomic scale and are significant when the fluid is constrained as a thin film between mineral grains (Horm 1990; Israelachvili 1991). Long range forces include van der Waals and electrical double-layer forces. Capillary and hydration forces are "short range" forces and result from the structural arrangement or ordering of water molecules in the thin film. On the other hand, Vigil et al. (1994) have recently proposed that the interfacial properties of quartz are not due to hydration effects but to the presence of a ~ 1 nm thick gel-like layer or silanol and silicilic acid groups on its surface.

High pressure and temperature are expected significantly to modify the forces and probably reduce the thickness of thin aqueous films (e.g., Heidug 1995). The slow transport rates observed in this study demonstrate that if a thin film is present between the grains of enstatite or forsterite, the diffusion rate through this film is much less than that for ionic diffusion in bulk water at similar conditions (e.g., Rubie 1986). When a sample is annealed in a fluid containing an isotopic tracer, the water has to migrate into sample during the anneal, whereas for rim formation water is incorporated during growth and presumably has an equilibrium concentration for the conditions of the experiments.

The slow rate of Si volume diffusion compared to that of Mg (e.g., Houlier et al. 1990; Chakraborty et al. 1994) is probably related to its high charge, which more than compensates for its small ionic radius, and this rate is enhanced by water or water-related defects in a crystal. A grain boundary is a less ordered region and water or related defects in this region may be less important for grain boundary diffusion that they are for volume diffusion in a highly ordered and neutrally charged crystal.

An important question is whether there is a significant difference in grain boundary diffusion rates along grain versus inter-phase boundaries for dry and water-present conditions. (This assumes that the interfacial angle (θ) is not reduced below 60° and hydrofracturing has not occurred.) Grain boundary diffusion rates of oxygen in water-saturated quartz-feld-spar agrregates are < 30 times faster than those in monomineralic aggregates (Farver and Yund 1995b). The activation energies for diffusion in the monomineralic and polymineralic aggregates are similar. These results together with the results for single pyroxene rims (this study) and pyroxene plus spinel rims (Liu et al., this issue) suggest that the effect of water is similar for interphase and grain boundaries. This is important because estimation of grain boundary transport rates during geological processes would be simplified even if the water content of rocks varied during the interval of interest.

Comparison with other grain boundary diffusion data

Fisler and Mackwell (1994) measured rim growth of fayalite between FeO and SiO_2 at one atmosphere using CO/CO_2 gas mixtures to control the oxygen fugacity (fo_2) and observed that rim growth rates decreased with increasing fo_2. Their calculated diffusivities for $D'_{Fe}\delta$ and $D'_{O}\delta$ (assuming Si is immobile) are within a factor of two (Fe is faster), and their data agree better with the predicted value for $D'_{O}\delta$. The value of $D'_{Fe}\delta$ for Fa_{100} can be obtained by extrapolating the data of Hermeling and Schmalzried (1984) for Fo_{10}–Fo_{80} and this extrapolated value agrees with Fisler and Mackwell's (1994) predicted value. The principal reason Fisler and Mackwell (1994) believe that O and not Fe is the rate-controlling diffusing species is because Hermeling and Schmalzried (1984) found that $D'_{Fe}\delta$ increases with fo_2. Fisler and Mackwell's (1994) data for $D'_{O}\delta$ are shown by the line labeled O (Fa) on Fig. 4. There is a very large difference in the activation enrgy for $D'_{O}\delta$ for fayalite (540 kJ/mole) compared to the values for feldspar (78 kJ/mole) and quartz (113 kJ/mole). However, it should be noted that the feldspar and quartz activation energies were determined at 100 MPa water pressure and the dominant oxygen-bearing species is thought to be H_2O (Farver and Yund 1995a).

Joesten and Fisher (1988) estimated silica grain boundary diffusion rates from wollastonite rims which grew on chert nodules when a limestone was heated by a nearby igneous intrusion. Based on heat flow estimates and measurements of the rim thicknesses, they estimated the silica grain boundary diffusion rates shown as SiO_2 (Wo) on Fig. 4. Clearly these data indicate much faster silica diffusion than those derived from the enstatite and forsterite rim growth experiments. This difference could

be real although the crystal structures of wollastonite and enstatite are related, suggesting they might have similar grain boundary diffusivities.

One possible explanation for the relatively fast silica diffusivities for natural wollastonite is that the wollastonite rims were porous. Alternatively the H_2O/CO_2 fluid may have produced interconnected channels for diffusion by reducing the liquid/solid interfacial angle. The effect of such a microstructure on bulk diffusion rates has been demonstrated using chloride solutions to produce inter-connected channels in quartz (Farver and Yund 1992). Such a microstructure might not be preserved if the wollastonite later equilibrated with a fluid of a different composition.

Direct comparison between grain boundary diffusion data obtained using an ion microprobe and rim growth experiments cannot be made because the former measures the diffusivities for individual ions whereas the rim method involves coupled diffusion of one or more cations together with oxygen, or interdiffusion of Mg and Si. Thus a comparison between the methods could not be made even if it was known whether MgO, SiO_2 or Mg_2Si_{-1} was the diffusing component during growth of these rims. However, if the diffusing component can be determined for rim growths such as these (R. Joesten, manuscript in preparation), the diffusivities for the individual ions could be determined using the ion microprobe. This would allow a very important comparison between individual ion diffusivities and their coupled diffusion rate. Coupled diffusion or interdiffusion is more important for evaluating reaction rates during high temperature metamorphism.

Although the diffusing components in the rim growth experiments reported here are presently unknown, it is still interesting to compare $D'_A\delta$ values for the forsterite aggregate with $D'_{Mg}\delta$ determined using the ion microprobe for forsterite aggregates (Farver et al. 1994). The diffusion rate for the vacuum-dried forsterite sample (solid square) is nearly 10^2 times faster than $D'_{Mg}\delta$ for the driest ion probe sample annealed in a Ca + CO_2 gas mixture. The diffusion rate for the wetter (0.1 wt % water added) forsterite rim sample (solid circle) is over 10^2 times faster than $D'_{Mg}\delta$ for the probe sample annealed at 1 atmosphere in an H_2 + CO_2 gas mixture. Although the water fugacity in the 0.1 wt % water-added rim samples is not known because the sample was not saturated with water, this situation probably corresponds to a higher water fugacity than that for the ion probe sample annealed in an H_2 + CO_2gas mixture. A comparison can also be made between the data for oxygen diffusion in fayalite rims (Fisler and Mackwell 1994) and the ion probe data (Fig. 4). These two sets of experiments were done in a CO + CO_2 gas mixture at one atmosphere, and $D'_{Fe}\delta$ is within a factor of two of $D'_O\delta$ for the fayalite experiments. The agreement for this comparison is good at the temperatures investigated, but the reported activation energies are quite different: 376 kJ/mole for the ion probe data versus 540 kJ/mole for the fayalite rim experiments.

When comparing data from different samples and sources it is important to recognize that either the grain boundary diffusion coefficient or the effective grain boundary width, or both, may differ from one situation to another. Recent studies have indicated, however, that synthetic and natural grain boundary widths are relatively narrow and a value between one and a few nm appears likely for many oxides and silicates (e.g., Joesten 1991) unless the minerals are highly altered. Furthermore and most importantly, values of $D'\delta$ for carefully hot-pressed aggregates with very low porosities are essentially identical with those obtained using natural fine-grained aggregates of quartz and albite (Farver and Yund 1992, Farver et al. (1994) 1995a). If thermal cracking or grain growth contributed significantly to the length of an ion probe diffusion profile, the $D'\delta$ values would be larger than those from rim growth experiments. The present study demonstrates that the effective width of grain boundaries is not a function of the confining pressure at which an enstatite aggregate is formed, at least not between about 450 and 1400 MPa. Therefore it appears that experimental grain boundary diffusion data should be applicable for predicting pervasive transport through rocks at metamorphic conditions.

Concluding statement

The major demonstration of this study is that grain growth rates involving enstatite and forsterite can be measured at high pressure and temperature and the rates are diffusion controlled, although the rate limiting diffusing component is unknown and could be MgO, SiO_2 or Mg_2Si_{-1}. The calculated diffusion rates are similar for enstatite and forsterite rims when about 0.1 wt % or more water is present. The diffusion rate for very dry enstatite is only slightly lower (factor of five), but for forsterite rims growing in vacuum-dried samples the diffusion rate is about 1/28 of the rate for samples with 0.1 wt % . Although the effect of water on grain boundary diffusion rates is not the same for enstatite and forsterite, the presence of water does not enhance the diffusion rates by several orders of magnitude as previously suggested (e.g., Rubie 1986). Confining pressures from 210–1400 MPa have no measurable effect on the diffusion rate through enstatite rims, but the nucleation rate is greatly reduced at low confining pressure when ≤1.0 wt % water is present, and this limits the experimental conditions at which rim growth rates can be measured.

Until the diffusing component can be identified, direct comparisons with other grain boundary diffusion rates are not possible. Nevertheless, the rates for the actual diffusing component are approximately consistent with grain boundary diffusion data obtained by other methods. If the diffusing component during rim growth can be identified, then the diffusion rates for the individual ions of the component (MgO, SiO_2 or Mg_2Si_{-1}) can be determined using the ion microprobe and these can be compared with the coupled or interdiffusion rates. This

would greatly increase our knowledge of grain boundary diffusion rates which are relevant to many geological situations involving compositional exchange.

Acknowledgements This research was supported by a grant from the National Science Foundation (EAR-9204785). I thank M. Liu, J. Tullis, and J. Farver for many helpful comments and suggestions during the course of this study and D. Fisler for a review of an earlier version of this manuscript. I especially want to acknowledge Ray Joesten who helped to set me straight on what is required to determine the diffusing component in rim growth experiments. Any remaining erroneous interpretations are solely mine. I also thank Prof. F. Seifert for providing the opportunity to visit the Geoinstitut in Bayreuth Germany where some of the early experiments were carried out.

Reference

Brady JB (1983) Intergranular diffusion in metamorphic rocks. Am J Sci 283A: 181–200

Brady JB (1995) Diffusion data for silicate minerals, glasses, and liquids. In: Ahrens T (ed) A Handbook of Physical Constants, AGU Reference Shelf 2, Am Geophys Union, Washington DC, pp 269–290

Brindley GW, Hayami R (1965) Kinetics and mechanism of formation of forsterite (Mg_2SiO_4) by solid state reaction of MgO and SiO_2. Philos Mag 12: 505–514

Carlson WD, Lindsley DH (1988) Thermochemistry of pyroxenes on the join $Mg_2Si_2O_6$–$CaMgSi_2O_6$. Am Mineral 73: 242–252

Chakraborty S, Farver JR, Yund RA, Rubie DC (1994) Mg tracer diffusion in synthetic forsterite San Carlos olivine as a function of *P, T,* and fo_2. Phys Chem Miner 21: 489–500

Douce AEP, Beard JS (1994) H_2O loss from hydrous melts during fluid-absent piston cylinder experiments. Am Mineral 79: 585–404

Evans BW, Guggenheim S (1988) Talc, pyrophyllite, and related minerals. In: Bailey S (ed) Hydrous phyllosilicates. (Reviews in mineralogy, 19) Mineral Soc Am, Washington, DC, pp 225–294

Farver JR, Yund RA (1990) The effect of hydrogen, oxygen, and water fugacity on oxygen diffusion in alkali feldspar. Geochim Cosmochim Acta 54: 2953–2964

Farver JR, Yund RA (1990) The effect of hydrogen, oxygen, and water fugacity on oxygen diffusion in alkali feldspar. Geochim Cosmochim Acta 54: 2953–2964

Farver JR, Yund RA (1990) The effect of hydrogen, oxygen, and water fugacity on oxygen diffusion in alkali feldspar. Geochim Cosmochim Acta 54: 2953–2964

Farver JR, Yund RA (1991a) Oxygen diffusion in quartz: dependence on temperature and water fugacity. Chem Geol 90: 55–70

Farver JR, Yund RA (1991b) Measurement of oxygen grain boundary diffusion in natural, fine-grained quartz aggregates. Geochim Cosmochim Acta 55: 1597–1607

Farver JR, Yund RA (1992) Oxygen diffusion in a fine-grained quartz aggregate with wetted and nonwetted microstructures. J Geophys Res 97: 4017–4029

Farver JR, Yund RA (1995a) Grain boundary diffusion of oxygen, potassium and calcium in natural hot-pressed feldspar aggregates. Contrib Mineral Petrol 118: 340–355

Farver JR, Yund RA (1995b) Inter-phase boundary diffusion of oxygen and potassium in K-feldspar/quartz aggregates. Geochim Cosmochim Acta 59: 3697–3706

Farver JR, Yund RA, Rubie DC (1994) Magnesium grain boundary diffusion in forsterite aggregates at 1000-1300°C and 0.1 MPa to 10 GPa J Geophys Res 99: 19809–19819

Fisher GW (1978) Rate laws in metamorphism. Geochim Cosmochim Acta 42: 1035–1050

Fisler DK, Mackwell SJ (1994) Kinetics of diffusion-controlled growth of fayalite. Phys Chem Miner 21: 156–165

Gee ML, Healy TW, White LR (1990) Hydrophobicity effects in the condensation of water films on quartz. J Colloid Interface Sci 140: 450–465

Gifkins RC (1970) Optical microscopy of metals. Elsevier, New York

Heidug WK (1995) Intergranular solid-fulid phase transformations under stress: the effect of surface forces. J Geophys Res 100: 5931–5940

Hermeling J, Schmalzried H (1984) Tracerdiffusion of the Fe-cations in olivine (Fe_xMg_{1-x}) SiO_4(III). Phys Chem Miner 11: 161–166

Holland TJB, Powell R (1990) AN enlarged and updated internally consistent thermodynamic dataset with uncertainties and correlations: the system K_2O-Na_2O-CaO-MgO-MnO-FeO-Fe_2O_3-Al_2O_3-TiO_2-SiO_2-C-H_2-O_2. J Metamorphic Geol 8: 89–124

Horm RG (1990) Surface forces and their action in ceramic materials. J Am Cerma Soc 73: 1117–1135

Houlier B, Cheraghmakani M, Jaoul O (1990) Silicon diffusion in San Carlos olivine. Phys Earth Planet Inter 62: 329–340

Huebner JS (1971) Buffering techniques for hydrostatic systems at elevated pressures. In: Ulmer GC (ed) Research techniques for high pressure and high temperature. Springler-Verlag, Berlin Heidelberg New York, pp 123–178

Israelachvili J (1991) Intermolecular surface forces, 2nd edn. Academic Press, San Diego, Calif

Joesten R (1991) Grain-boundary diffusion kinetics in silicate oxide minerals In: Ganguly J (ed) Diffusion, atomic ordering, mass transport: selected problems in geochemistry (Advances in physical geochemistry, 9) Springer-Verlag, Berlin Heidelberg New York, pp 347–397

Joesten R, Fisher G (1988) Kinetics of diffusion-controlled mineral growth in the Christmas Mountains (Taxas) contact aureole. Geol Soc Am Bull 100: 714–732

Kronenberg AK, Kirby SH, Aines RD (1986) Solubility and diffusional uptake of hydrogen in quartz at high water pressure; implications for hydrolytic weakening. J Geophys Res 91: 12723–12744

Liu M, Yund RA (1992) NaSi-CaAl interdiffusion in plagioclase. Am Mineral 77: 25–283

Liu M, Peterson J, Yund RA (1996) Diffusion-controlled growths of albite and pyroxene reaction rims. Contrib Mineral Petrol (this issue)

Nitsan U (1974) Stability field of olivine with respect to oxidation reduction. J Geophys Res 79: 706–711

Nowotny J (1991) Interface defect chemistry of oxide ceramic materials: unresolved problems. Solid State Ionics 49: 119–128

Parks GA (1990) Surface energy adsorption at mineral-water interfaces: an introduction. In Hochella M Jr, White AF (eds) Mineral-water interface geochemistry. (Reviews in mineralogy, 23) Mineral Soc Am, Washington, DC, pp 133–175

Rosss NL, Navrotsky A (1978) The Mg_2GeO_4 olivine-spinel transition. Phys Chem Miner 14: 473–481

Rubie DC (1986) The catalysis of mineral reactions by water restrictions on the presence of aqueous fluid during metamorphism. Mineral Mag 50: 399–415

Schmalzried H (1978) Reactivity and point defects of double oxides with emphasis on simple silicates. Phys Chem Miner 2: 279–294

Shatynski SR, Hirth JP, Rapp RA (1976) A theory of multiphase binary diffusion. Acta Metall 24: 1071–1078

Vigil G, Xu Z, Steinberg S, Israelachvili J (1994) Interaction of silica surfaces. J Colloid Interface Sci 165: 367–385

Walther JV, Wood BJ (1984) Rate and mechanism in prograde metamorphism. Contrib Mineral Petrol 88: 246–259

Watson EB (1986) An experimental study of oxygen transport in dry rocks and related kinetic phenomena. J Geophys Res 91: 14117–14131

Wegner MW, Christie JM (1985) General chemical etchants for microstructural defects in silicates. Phys Chem Miner 12: 90–92

Yund RA, Tullis J (1992) Effect of water on grain boundary diffusion rates. Eos Trans AM Geophys Union 73:373–374